Swimming Motion Control for Biometric Fish Robot by Utilizing Turning Coefficient

Yoong Hou Pin
yoongpin@ums.edu.my

Lin Boon Hoe
mydaniel86@yahoo.com

Kenneth Teo Tze Kin
kenteo@ums.edu.my

Ismail Saad
ismail_s@ums.edu.my

School of Engineering & IT
Universiti Malaysia Sabah
Kota Kinabalu, Malaysia

***Abstract* — In this paper turning coefficient had been utilize for the swimming motion equation of a biometric fish robot. The swimming equation based on Carangiform Wave is cascaded with the arc equation to change the oscillating axis during turning movement (Chao Zhou). Usually turning movement is generated by defining the turning radius of the arc equation to bend the Carangiform oscillating axis. This involves the computation of turning radius power of two and infinite radius value during straight movement. Thus turning coefficient had been introduced to the arc equation to simplify the computation process and the turning coefficient can set as zero during straight movement. With the implementation of turning coefficient, the turning radius is fixed at a minimum value. This reduces the computational time of about 9% and maintaining the ability to perform smooth turning movement. Infrared sensor provides environment feedback for altering the turning coefficient linearly. The rate of change for the turning coefficient can be adjusted to define the sensitivities of the fish reacting to the environment.**

Keywords-Carangiform; turning coefficient; fish robot

I. INTRODUCTION

The fish swimming ability both in efficiency, maneuverability and low noise had been perfected through the evolution and natural selection process for billions of years. This swimming ability had inspire many scientists to also evolve the propeller propulsion system of Autonomous Underwater vehicle (AUV) into undulating body and fin. By doing so, the power pack size on board the AUV can be reduced and also lower the noise generation underwater. Because of the advantages with fish swimming motion, many fish like underwater robot had been studied and developed since the first RoboTuna was developed at MIT in 1998 [1]. Robot fish can be applied in oil leak detection, underwater repair, construction work and underwater mining. Due to the low noise and fish mimicking feature, the fish robot become the best tool for marine fauna habitat observation.

Thus, a robot fish with Carangiform swimming pattern had been developed in the lab at Sabah, Malaysia. This fish robot development covers the kinematics and dynamic model, control system control circuit, and hardware. However, this paper only emphasize on the new method developed for motion generation utilizing turning coefficient. Many researchers [1, 4, 6] had developed the swimming motion by adopting Carangiform developed by Sir Michael J. L. in the early 1970. The Carangiform model consist of an oscillating wave and an envelope equation. The model is then added with an arc equation to bend the oscillating axis to perform turning motion [2, 7, 8].

The used of arc equation increase the model complexity and, thus, increase computational time which affects the real time calculation. During straight swimming movement the turning radius become infinite value, this again burdens the computation system. The purpose of utilizing the turning coefficient is to reduce the computational complexity and avoid in using infinite turning radius during straight swimming motion.

To utilize turning coefficient, turning radius of the arc equation is fix at the minimum, which is 0.25m for this fish robot. During straight swimming movement turning coefficient is set at zero to eliminate the arc equation and during minimum turning radius turning coefficient is set to one. Infrared sensor is developed to provide obstacle feedback for altering the turning coefficient. The rapid increase of turning coefficient indicates the fish robot sensitivities reacting to the environment.

The utilization of turning coefficient is able to reduce the computational time to about 9%. The control system also made easy by alter the turning coefficient from zero to one, instate of turning radius from 0.24m to infinity.

This paper is organized as follow. The related work on the robot fish swimming motion using Carangiform is described in Section II. The derivation of Carangifrom wave equation utilizing turning coefficient is described in Section III. The next section will discuss the differences of the proposed method and conventional method. In the following section describe the control of turning coefficient by the feedback sensor. Result of utilizing the turning coefficient is then presented in Section VI.

978-0-7695-4336-9/11 $26.00 © 2011 IEEE
DOI 10.1109/ISMS.2011.76

IEEE computer society

Finally, concluding remarks are provided in Section VII.

II. Related Work

The general Carangiform fish swimming motion equation (1) suggested by Sir Michael J. L. consist of a wave envelop and an oscillating wave. This equation had been adopted by many research like [1, 2, 3, 4, 5].

$$y_{body}(x,t) = (c_1 x + c_2 x^2)\sin(kx + \omega t) \quad (1)$$

where y_{body} is transverse displacement of tail unit; x is the displacement along main axis; $k = \frac{2\pi}{\lambda}$ is the wave number; λ is the wave length; c_1 is the linear wave amplitude envelope; c_2 is the quadratic wave amplitude envelope; $\omega = 2\pi f$ is wave frequency; and t is time. Equation (1) is later simplified to model a serial N-joint oscillating mechanism as equation (2) by 9].

$$y_{body}(x,i) = (C_1 x + C_2 x^2)\sin\left(kx + \frac{2\pi}{M} i\right), i \in [0, M-1] \quad (2)$$

Where i is the serial number in an oscillation cycle; M is the resolution of discrete travelling wave. The simplification eases the forming of algorithm in calculating real time joint angle for swimming motion control.In [8] equation (1) is added with an arc equation to bend the oscillating axis to perform turning movement. The direction of turning is specified by the arc equation polarity. Thus the total swimming motion equation is written as (3).

$$y_{body}(x,i) = (c_1 x + c_2 x^2)\sin(kx + \omega t) + \sqrt{R^2 - x^2} - R \quad (3)$$

Where R is the turning radius of the tail axis. Figure 1, illustrate the Carangiform wave generated by equation (3) with turning radius of 0.40m.

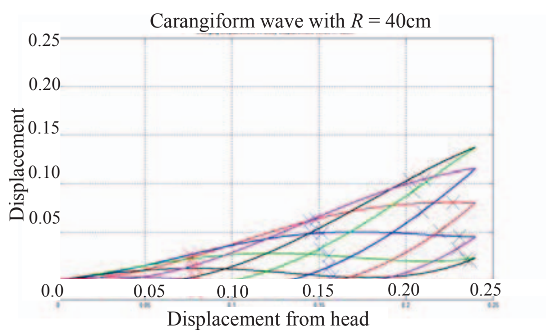

Figure 1. Carangiform wave with 0.40m turning radius.

Equation (3) is effective during small turning radius. However, it becomes not effective during straight movement. This due to the turning radius R has to be very larger compared to x for the elimination of arc equation.

III. Swimming Motion Equation with Turning Coefficeint

The equation (2) and (3) is combined and adopted to yield the total swimming motion equation. This is due to equation (2) provide the discrete platform to ease the algorithm formation and equation (3) provide turning ability. However, the arc equation involves computation of power two for large number during turning movement at large turning radius or straight movement. Thus, turning coefficient T is utilized in equation (3) to control the amount of turning and it is rewritten as equation (4)

$$y_{body}(x,i) = (C_1 x + C_2 x^2)\sin\left(kx + \frac{2\pi}{M} i\right) + T\sqrt{0.0625 - x^2} - 0.25 \quad (4)$$

Turning radius R is substituted with the smallest value, which is 0.25m. Turning coefficient T can be varying from 0 to 1 for controlling the fish robot turning. Figure 2. Illustrate the Carangiform wave generated by equation (4) with T = 0.6, which is equivalent to R = 0.40m.

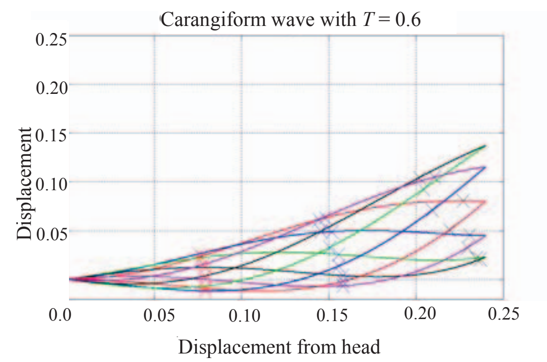

Figure 2. Carangiform wave with turning coefficient T = 0.6.

There is no significant difference shown in Figure 1 and Figure 2. However, detail of corresponding turning radius and turning coefficient will be study in the next section.

IV. Turning Radius Coresponse with Turning Coefficient

A. *Turning Coefficient and Turning Radius*

The turning radius with respect to the corresponding turning coefficient is formulated by equating the two arc equation as per (5)

$$T\sqrt{0.0625 - x^2} - 0.25 = \sqrt{R^2 - x^2} - R \quad (5)$$

The turning coefficient from 0.1 to 0.9 with every step of 0.1 is substituted into equation (5) to obtain the corresponding *R* value, throughout the fish body length *x*. The *R* value is then averaged in obtaining the corresponding R_{avg}. Table 1, shows the *T* value and the corresponding R_{avg} value.

TABLE 1, THE TURNING COEFFICIENT T WITH CORRESPONDING AVERAGE TURNING RADIUS R_{avg}.

Turning Coefficient *T*	Average Turning Radius R_{avg} (m)
1	0.25000
0.9	0.27587
0.8	0.30696
0.7	0.34692
0.6	0.30021
0.5	0.37382
0.4	0.58672
0.3	0.77323
0.2	1.14625
0.1	2.26530
0	∞

Here *T* is fixed to obtain the corresponding *R* instate of fixing the *R* to obtain the corresponding *T*. This is due to the feedback altering the Turning coefficient instate of turning radius. The nonlinear relationship between *T* and R_{avg} is shown in Figure 3.

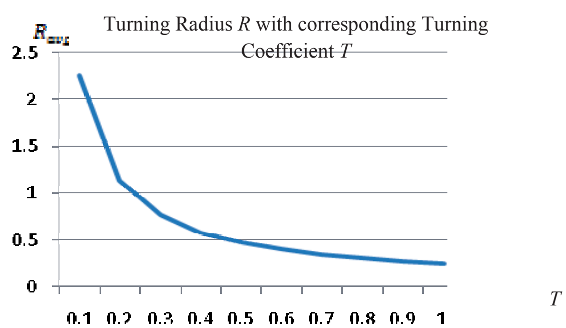

Figure 3, Average turning radius R_{avg} with corresponding turning coefficient *T*

B. Error Cuase by Turning Coefficient

By implementing the turning coefficient, the oscillating axis has became a fraction of an arc with 0 < *T* < 1 and only at *T* = 1 has a perfect arc. The error e_T for the arc using turning coefficient and the arc equation at each corresponding radius can be obtained as equation (6)

$$e_T = \sqrt{R_{avg}^2 - x^2} - T\sqrt{0.0625 - x^2} + 0.25 - R_{avg} \quad (6)$$

The error e_T is computed and statically analyzed by obtaining the average and standard deviation. The result will be discussed in section VI.

V. FEEDBACK AND FISH SENSITIVITES

Three infrared sensors is mould on the fish robot head to sense obstacle. One facing the front another two facing the left and the right. Figure 4, Illustrates the position of the infrared sensor.

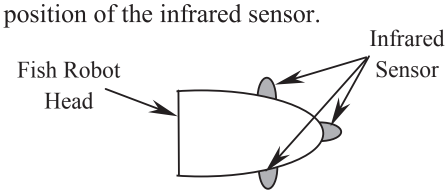

Figure 4, Top view of fish robot head and infrared sensor position.

The sensor feedback is utilized to alter the turning coefficient in the control algorithm. Table 2 shows the set of rules programmed in the algorithm for making direction decision when the fish senses obstacle. The rule directs the fish away from the obstacles by turning to the opposite direction of the obstacles. When the fish senses obstacles at all the sensors it will only turn right.

TABLE 2. DIRECTION DECISION TABLE

Obstacle left	Obstacle center	Obstacle right	Turn left	Go straight	Turn right
0	0	0		1	
0	0	1	1		
0	1	0	1		
0	1	1	1		
1	0	0			1
1	0	1		1	
1	1	0			1
1	1	1			1

The polarity of *T* value indicates the turning direction. For negative *T* value the arc will fall under the negative zone, which the robot will turn right and vice versa. The decision table provides the direction for the fish to turn. If the direction is right the *T* value will be continuously decreased with 0.1 per iteration until -1 while the obstacle persists. Meanwhile for the straight movement, the algorithm will shift the *T* value back to zero with the rate of 0.1 per iteration.

The rate of changing of *T* value can be denoted as sensitivities of the fish robot. By considering the relation between the turning coefficient and the turning radius, the robot fish is found to have exponential sensitivities.

VI. Results

A. Error Tabulation

The first result presented is the error for the arc using turning coefficient compared to the arc equation. This will verify the applicability of utilizing turning coefficient. The Table 3 shows the calculated result for the arc error, standard deviation and averge error percentage. Average error percentage for the arc through all turning coefficient is found to be lower than 0.1 percent. The average error achieves highest value of about 0.3mm and with the highest standard of deviation of 9.85mm. This result had shown the feasibility of utilizing turning coefficient. However, the standard deviation had showed the error is scatted about 6% at $T = 0.8$.

Table 3. Arc Average Error, Standard Deviation and Error Percentage.

T	Average Turning Radius	Average Error	Std. Deviat'n	Error (%)
1	0.25000	0.00000	0.00000	0.00000
0.9	0.27315	0.00025	0.00788	0.09043
0.8	0.30152	0.00027	0.00958	0.08855
0.7	0.33877	0.00026	0.00985	0.07616
0.6	0.38933	0.00024	0.00933	0.06062
0.5	0.46122	0.00021	0.00831	0.04445
0.4	0.57040	0.00017	0.00697	0.02963
0.3	0.75419	0.00013	0.00540	0.01710
0.2	1.12419	0.00009	0.00368	0.00775
0.1	2.24083	0.00004	0.00186	0.00196

Due to the scatted error, further analysis is carried out to show the error tabulation. The average error at distance along the fish body is computed to illustrate the error tabulation. Figure 4 shows the error tabulation obtain by averaging the error at consecutive distance of the fish body.

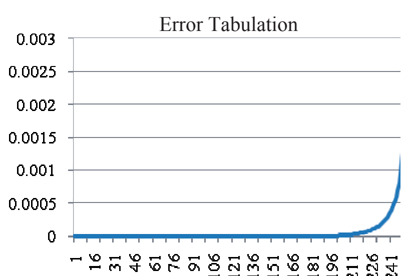

Figure 4. Error tabulation

The error tabulation showed the increase of error at the end of the fish body. However, the biometric fish robot had three joint and each is 80mm apart. Thus, the last joint is located at 180mm away from the head. It falls in the region where error is negligible. Only the tip of the tail fin will have an error up 6%. With this, again the used of turning coefficient had been verified.

B. Algorithm Loop Time

Experiment had been set up to verify the simplification can to reduce the computational time. Two swimming motion algorithm one using turning coefficient and another using normal arc equation is programmed into a PIC 18F14K50 Microcontroller. Every loop cycle the algorithm will toggle an output pin. Measuring the toggling frequency, the algorithm loop time using turning coefficient is found to be 81.3ms and the loop time using conventional arc equation is 88.6ms. Thus, a total time saving of 9.2% is achieved utilizing turning coefficient in the swimming motion generation. The short loop time is necessary for the real time computation. The utilization of turning coefficient in swimming motion had improved the system loop time and improve the real time control

C. Swimming Motion Generation

The last part of the result presented the implementation of the turning coefficient in generating the fish movement. The Figure 5 shows the turning movement had been successfully generated for turning action.

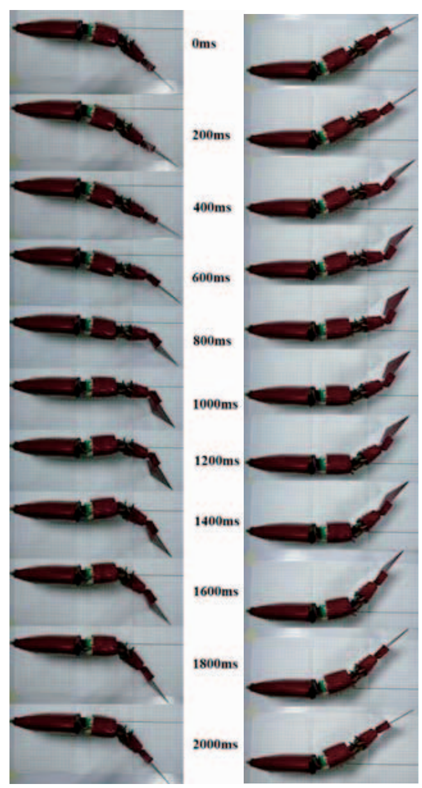

Figure 5. Turning movement generated by utilizing turning coefficient

VII. Conclusion and Future Work

In this paper, turning coefficient had been successfully utilized in the fish swimming motion equation. The system shows no significant error, thus, this verified the utilization of turning coefficient. This method had yield 9.2% of time saving for algorithm loop time by simplifying the computation of swimming motion equation. Physical hardware had been developed and turning coefficient is implemented successfully in generating the swimming motion for a fish robot.

In future, point to point transformation will be developed to incorporate with the swimming motion and the hydrodynamic of the fish robot to perform point to point maneuvering. The real fish sensitivities can be further understood and modeled into the robot fish. This will provide the survivor ability of the fish robot during it operation in the underwater environment. The last part of work is to water proof the system for real environment application.

Acknowledgment

The author wish to thank Universiti Malaysia Sabah, Center of Research and Innovation, School of Engineering & IT and Centre of Materials & Minerals.

References

[1] J. Lui, H. Hu, "A 3D Simulator for Autonomous Robotic Fish" Int. Journal of Automation and Computing 1, 2004, pp 42-50.

[2] J. Lui, I. Dukes, R. Knight, H. Hu, "Development of Fish-Like Swimming Behaviours for an Autonomous Robotic Fish" Control, University of Bath. 2004, ID-217.

[3] J. Guo, "Maneuvering and Control of a Biomimitic Autonomous underwater Vehicle" Auton Robot, 2009, Vol. 26 pp 241-249.

[4] J. Yu, M. Tan, S. Wang and E. Chen, " Development of a Biomimetic Robotic Fish and Its Control Algorithm" IEEE Trans. on System, Man and Cybernetics, 2004, Vol. 34, No. 4.

[5] D. Barrett, M. Grosenbaugh, M Triantafyllou, "The Optimal Control of a Flexible Hull Robotic Undersea Vehicle Propelled by an Oscillating Foil. IEEE Exploer, Proceedings of Symposium on Autonomous Underwater Vehicle Technology, 1996, pp 1-9.

[6] K. A. Morgansen, et al. "Nonlinear Control Methods for Planar Corangiform Robot Fish Locomotion" IEEE, International Conference on Robotics & Automation, 2001, pp 427-434.

[7] H. Hu, J. Liu, I. Dukes and G. Francis, "Design of 3D swim Patterns for Autonomous Robot Fish" IEEE, International Conference on Intellegent Robots and Systems. 2006, pp 2406-9321.

[8]C. Zhou, et. al. " The Posture Control and 3-D Locomotion Implementation of Biomimetic Robot Fish" IEEE, International Conference on Intelligent Robots and Systems" 2006, pp5406-5411.

[9] J. Yu, S. Wang, M. Tan, "A Simplified Propulsive Model of Bio-mimetic Robot Fish and Its Realization" Robotica, 2005, Vol. 23, pp 101-107.

[10] D. Mahammadshahi, et al. "Design, Fabrication and Hydrodynamic Analysis of a Biomimetic Robot Fish" International Journal of Machanics, 2008, Vol. 2, pp 59-66.

[11] J. E. Colgate, K. M. Lynch. "Mechanics and Control of Swimming: A Review" IEEE Journal of Oceanic Engineering, 2004, Vol. 29, No. 3.